ACCOUNTS of chemical research

pubs.acs.org/accounts Article

Foldaxanes: Rotaxane-like Architectures from Foldamers

Victor Koehler,[§] Arundhati Roy,[§] Ivan Huc,* and Yann Ferrand*

Cite This: *Acc. Chem. Res.* 2022, 55, 1074−1085 Read Online

ACCESS | Metrics & More | Article Recommendations

CONSPECTUS: Mechanically interlocked molecules such as rotaxanes and catenanes contain free-moving components that cannot dissociate and have enabled the investigation and control of various translational and rotational molecular motions. The architecture of pseudo-rotaxanes and of some kinetically labile rotaxanes is comparable to that of rotaxanes but their components are reversibly associated and not irreversibly interlocked. In other words, pseudo-rotaxanes may fall apart. This Account focuses on a peculiar family of rotaxane-like architectures termed foldaxanes.

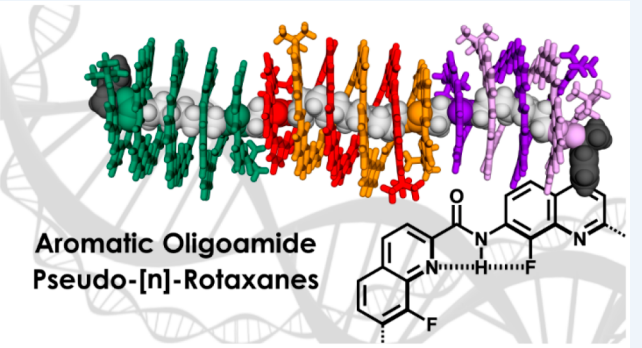

Foldaxanes consist of a helically folded oligomer wound around a rod-like dumbbell-shaped guest. Winding of the helix around the rod thus entails an unwinding−rewinding process that creates a kinetic barrier. It follows that foldaxanes, albeit reversibly assembled, have significant lifetimes and may not fall apart while defined molecular motions are triggered. Foldaxanes based on helically folded aromatic oligoamide hosts and oligo(alkyl carbamate) guests can be designed rationally through the inclusion of complementary binding motifs on the rod and at the inner rim of the helix so that helix length and rod length match. Single helical foldaxanes (bimolecular species) and double helical foldaxanes (trimolecular species) have thus been produced as well as poly[*n*]foldaxanes, in which several helices bind to long rods with multiple binding stations. When the binding stations differ and are organized in a certain sequence, a complementary sequence of different stacked helices, each matching with their binding station, can be assembled, thus reproducing in an artificial system a sort of translation process.

Foldaxane helix handedness may be controlled by stereogenic centers on the rod-like guest. Handedness can also be transmitted from helix to helix in polyfoldaxanes. Foldaxane formation has drastic consequences for the rod properties, including its stiffening and the restriction of the mobility of a macrocycle already interlocked on the rod. Fast translation (without dissociation) of helices along rod-like guests has been demonstrated. Because of the helical nature of the hosts, translation may be accompanied by rotation in various sorts of screw-like motions. The possibility, on longer time scales, for the helix to dissociate from and reassociate to the rod has allowed for the design of complex, kinetically controlled supramolecular pathways of a helix on a rod. Furthermore, the design of helices with a directionality, that is, with two distinct termini, that bind to nonsymmetrical rod-like guests in a defined orientation makes it possible to also control the orientation of molecular motion. Altogether, foldaxanes constitute a distinct and full-of-potential family of rotaxane-like architectures that possess designer structures and allow orchestration of the time scales of various supramolecular events.

KEY REFERENCES

- Gan, Q.; Ferrand, Y.; Bao, C.; Kauffmann, B.; Grélard, A.; Jiang, H.; Huc, I. Helix-Rod Host-Guest Complexes with Shuttling Rates Much Faster than Disassembly. *Science* **2011**, *331*, 1172−1175.[1] *The rational design and self-assembly of foldaxanes based on aromatic oligoamide helices and alkyl dicarbamate rods and the demonstration of their pH-controlled shuttling motions without dissociation.*
- Gan, Q.; Wang, X.; Kauffmann, B.; Rosu, F.; Ferrand, Y.; Huc, I. Translation of Rod-like Template Sequences into Homochiral Assemblies of Stacked Helical Oligomers. *Nat. Nanotechnol.* **2017**, *12*, 447−452.[2] *The loading of stacks of single and double helices on rods that contain multiple binding stations according to helix−station complementarity so that the sequence of station and sequence of helix match and the transmission of stereochemical information through such systems.*
- Wang, X.; Wicher, B.; Ferrand, Y.; Huc, I. Orchestrating Directional Molecular Motions: Kinetically Controlled Supramolecular Pathways of a Helical Host on Rodlike Guests. *J. Am. Chem. Soc.* **2017**, *139*, 9350−9358.[3] *The*

Received: January 27, 2022
Published: March 16, 2022

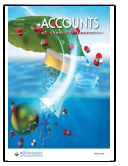

implementation of series of supramolecular events guided by the fast kinetics of threading a rod in a helix and the slow kinetics of winding a helix around a rod.

1. INTRODUCTION

Mechanically interlocked molecules have opened up considerable capabilities in molecular machinery.[4−7] For example, rotaxanes (Figure 1A) have emerged as an archetypical architecture enabling the controlled motion of rings mechanically bound to dumbbell-shaped molecular rods.[8−10] The moving parts of a rotaxane, the ring and the rod, cannot dissociate, and various strategies have been devised to produce such objects.[11] In contrast, pseudo-rotaxanes allow for the dissociation of their subcomponents because the rod is not dumbbell-shaped, thus allowing ring slippage (Figure 1B).[12] Kinetically labile rotaxanes have also been described (Figure 1C).[13−15] Pseudo-rotaxanes possess the advantage that they can be produced through self-assembly by simply mixing their components. Their existence rests on the ring affinity for the rod. However, they can dissociate, which makes their use in molecular machinery complicated: a machine preferably may not be allowed to fall apart to achieve work.

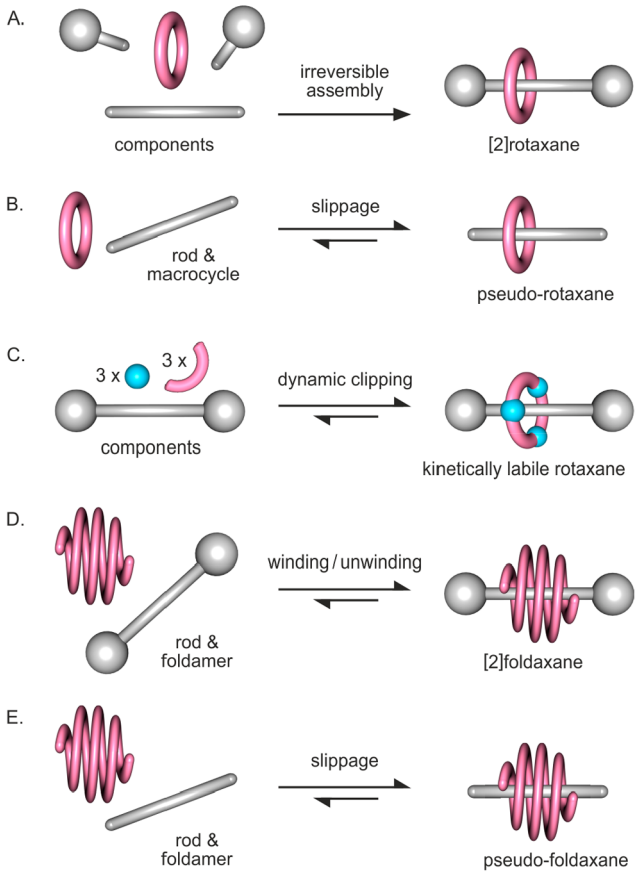

Figure 1. (A) Irreversible formation of a [2]rotaxane and (B−E) reversible formation of various types of architectures: pseudo-rotaxanes (B), kinetically labile rotaxanes (C), foldaxanes (D), and pseudo-foldaxanes (E).

This Account focuses on foldaxanes, a peculiar family of rotaxane-like architectures[16] in which the ring is replaced by a helically folded oligomer, that is, a foldamer[17−20] (Figure 1D). A one-turn helix may be assimilated to a ring closed by noncovalent interactions. It is a dynamic object but its time constants, for example, the rates at which it winds and unwinds, may substantially vary depending on its inherent rigidity and upon adding helix turns. Using stable helices, long-lived foldaxanes may be produced, that is, helix−rod complexes that do not dissociate while some molecular motions take place. Designing foldaxane structural characteristics thus enables the orchestration of the time scales of the various processes involved and creates new opportunities for controlling molecular motions.

The development of foldaxanes stemmed from the use of helical foldamers with sizable cavities as containers for molecular recognition.[21−28] While this background mostly concerns the recognition of guests small enough to entirely fit in a helix cavity, an increasing number of reports target rod-like guests that protrude from the helix, thus defining a foldaxane or pseudo-foldaxane architecture (Figure 1D,E). With few exceptions,[29,30] foldaxanes involve relatively rigid aromatic helices. Following early reports based on oligo(*meta*-phenylene ethynylene)s[31−33] and on naphthyridine oligomers,[34] a range of foldaxanes has been reported that exploit the modularity and synthetic access of aromatic oligoamide foldamers.[19,35−37] Depending on the properties of the foldamer host and the rod-like guest, single or double helical foldaxanes may be produced. Their design principles and their intriguing properties are presented in detail in the following.

2. SINGLE HELICAL FOLDAXANE DESIGN

Aromatic oligoamide foldamers adopt stable conformations such as helices or sheets that can be simply predicted because they constitute the direct outcome of local preferences at each rotatable bond that define the relative orientation of consecutive units.[33−35] Over the years, a toolbox of diamine, diacid, and amino acid heterocyclic aromatic monomers that differ by their size and the position of their amine and acid substituents have been developed. A sampling of these monomers is shown in Figure 2A, and typical interactions that govern backbone conformation are shown in Figure 2B. Depending on the monomer used, different strand curvatures may be imparted that will give rise to helical structures of varying diameter. For example, Q_n sequences (Figure 2B) form highly curved helices with no cavity. In contrast, Q^F_n sequences (Figure 2C) form less curved helices and possess a small cavity in which an alkyl chain may fit. Upon combining monomers that code for a wide helix diameter in the center of a sequence and short Q_n segments at both ends, a helical capsule can be produced that can completely seclude a guest molecule from the surrounding medium (Figure 2D).[19] Helical containers based on these principles have been shown to bind a broad range of guests, from anions[38] or cations[39] to organic acids[22,40] and carbohydrates.[41,42]

It was conceived that by removing the end-caps from a capsule sequence, that is, the highly curved extremities, guest molecules may be allowed to protrude from the helix to produce foldaxanes and pseudo-foldaxanes. Capsule sequence **1**[43] (Figure 3A) was selected for this purpose. It comprises two $P^NP^CP^N$ polar clefts that can hydrogen bond to a guest's polar function (Figure 3B), a central $Q^F_2A^FQ^F_2$ cylindrical cavity to accommodate a short alkyl chain, and terminal Q_3 caps that close the cavity. Sequence **1** was rationally designed to bind to guest molecules such as 1,4-butanediol or 4-amino-1-butanol and successfully does so (Figure 3E) with a K_a of ca. 10^3 L·

https://doi.org/10.1021/acs.accounts.2c00050
Acc. Chem. Res. 2022, 55, 1074−1085

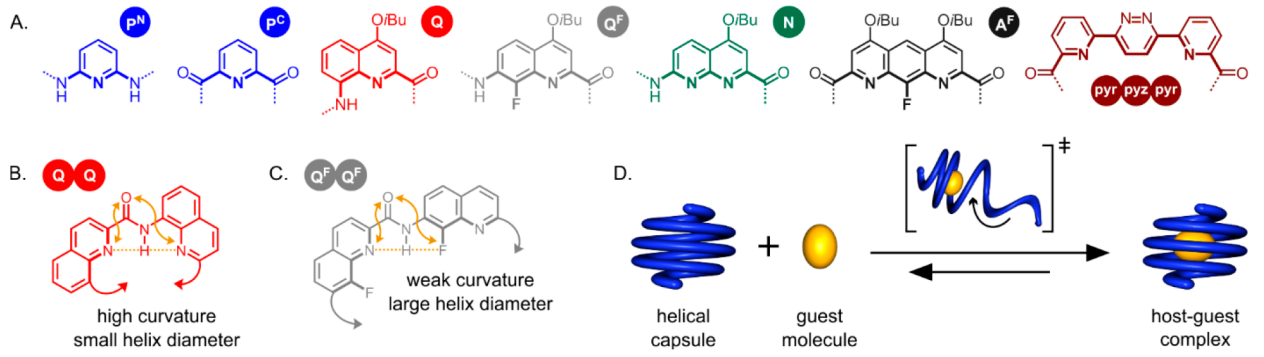

Figure 2. (A) Toolbox of heterocyclic amino acid, diacid, or diamine aromatic building blocks of helical aromatic oligoamide foldamers, and their letter and color codes. Folding principles of (B) Q_2 and (C) Q^F_2. Aryl-amide pseudoconjugation, hydrogen bonds (dashed lines), and electrostatic repulsions (arrows) contribute to the stabilization of a preferred conformation at each aryl-amide bond, giving rise to a helix in sufficiently long sequences. Intramolecular aromatic stacking comes as an additional, solvent dependent stabilizing force. (D) Encapsulation of a guest molecule (yellow sphere) in a molecular helical capsule (blue tube) possessing a reduced diameter at both ends, leading to a host−guest complex via a transient local unfolding of the helix.

mol^{-1} in chloroform.[41] Using **1** as a starting point, the two Q_3 caps were removed to let longer guests protrude from the cavity and allow for the binding of dumbbell-shaped molecules. Accordingly, sequences **2a−2d** are composed of a central cylindrical cavity $Q^F_mA^FQ^F_m$ of variable length, and all possess two $P^NP^CP^N$ hydrogen bond donor clamps. Gratifyingly, these foldamers were shown to bind *α,ω*-alkanediamine-derived dicarbamate guests, thus producing an ensemble of helix−rod complexes.[1,2] Thin guests such as **5** can thread themselves into the cavity (Figure 3B,F). Complexes also form with dumbbell-shaped guests such as **3** and **4** (Figure 3F), which involve another mechanism of formation. As depicted in Figure 1D, it is inferred that the helix must wind around the rod. However, aromatic oligoamide helices are particularly stable and may not completely unfold for this purpose.[44] A sort of screwing around the rod while the helix keeps its shape may be envisaged. Thus, bulky stoppers do not alter the binding energy (for example, see **2c⊃4b** vs **2c⊃5** in Figure 3D). However, bulky stoppers alter the binding and release mechanisms and thus the associated kinetics. Threading typically takes place rapidly and cannot be monitored by NMR, whereas winding may take days to reach equilibrium.[1,3]

The formation constants of foldaxanes made of different helix and rod lengths revealed two main trends (Figure 3D). First, a rather strict match between helix length and guest length is required for optimal binding. Removing or adding a single methylene unit within the rod may have drastic consequences on foldaxane stability. Second, foldaxane stability increases for longer helices and rods, which culminated with K_a = 345 000 $L{\cdot}mol^{-1}$ for **2d⊃3f**. This suggests that foldaxane stability is not solely determined by the hydrogen bonds between the carbamate and the $P^NP^CP^N$ polar clefts but that contacts between the alkyl chains and the fluorine atoms of Q^F and A^F units are also favorable.

Another aspect is that helices **2a−2d** bind selectively to dicarbamates of *α,ω*-alkanediamines. The $P^NP^CP^N$ polar clefts hydrogen bond to the carbamate carbonyl group, and binding affinities collapse if the carbamate orientation is inverted by swapping amino and oxy functions or if it is replaced by an amide or an ester. This selectivity offered the possibility to fine-tune the system. Thus, the P^NP^CN polar cleft, where the terminal pyridine was replaced by a naphthyridine, was designed to selectively recognize an amide instead of a carbamate (Figure 4).[45] The outcome is that dissymmetrical sequence **6**, which possesses both $P^NP^CP^N$ and P^NP^CN segments, selectively binds to dissymmetrical guests like **7c** with a K_a of 28 000 $L{\cdot}mol^{-1}$. Complexes with amide and carbamate mismatching the two polar clefts are transiently observed before disappearing below detection levels of ^1H NMR. Such complexes make it possible to control the relative orientation of the helix and the rod, a property that has been achieved with few rotaxanes.[46−49]

3. FOLDAXANES AND DOUBLE HELICES

The key modification to transform a capsule sequence such as **1** (Figure 3A,E) into a helix prone to foldaxane formation is the removal of the Q_3 segments that cap the helix cavity. Yet, this change has another consequence other than forming an open-ended helix. Helices with a wide diameter have a strong propensity to self-assemble into double helical dimers because of the lower energy cost of spring-like extension when helix diameter is larger, as for macroscopic metal springs.[50] Q_3 segments are more curved and disfavor this process (whereas Q_2 may accommodate it).[51] It follows that foldaxane assembly competes with double helix formation (Figure 3C). Nevertheless, despite the generally high stability of these double helices, this competition does not overwhelm foldaxane formation. The reason is that one double helix can dissociate to form two foldaxanes. The overall equilibrium is thus defined by the ratio between the constant of dimerization and the square of the constant of formation of the foldaxane from a single helix. Nevertheless, double helix formation complicates measurements. Because the single helix is involved in two equilibria, it is undetectable in NMR spectra at equilibrium. This makes it more difficult to directly measure the constant of formation of the foldaxane from the single helix. Instead, we calculate the constant of formation of two foldaxanes from the double helix (Figure 3C). Furthermore, the kinetics of double helix formation are slow, particularly so for long oligomers, and it may take days to bring foldaxane formation to equilibrium when mixing a rod guest and a double helix. Fortunately, a majority of the aromatic oligoamide strands can be precipitated in their out-of-equilibrium single helical form from methanol. Producing foldaxanes from the single helix is much faster, and equilibrium is reached rapidly.

https://doi.org/10.1021/acs.accounts.2c00050
Acc. Chem. Res. 2022, 55, 1074−1085

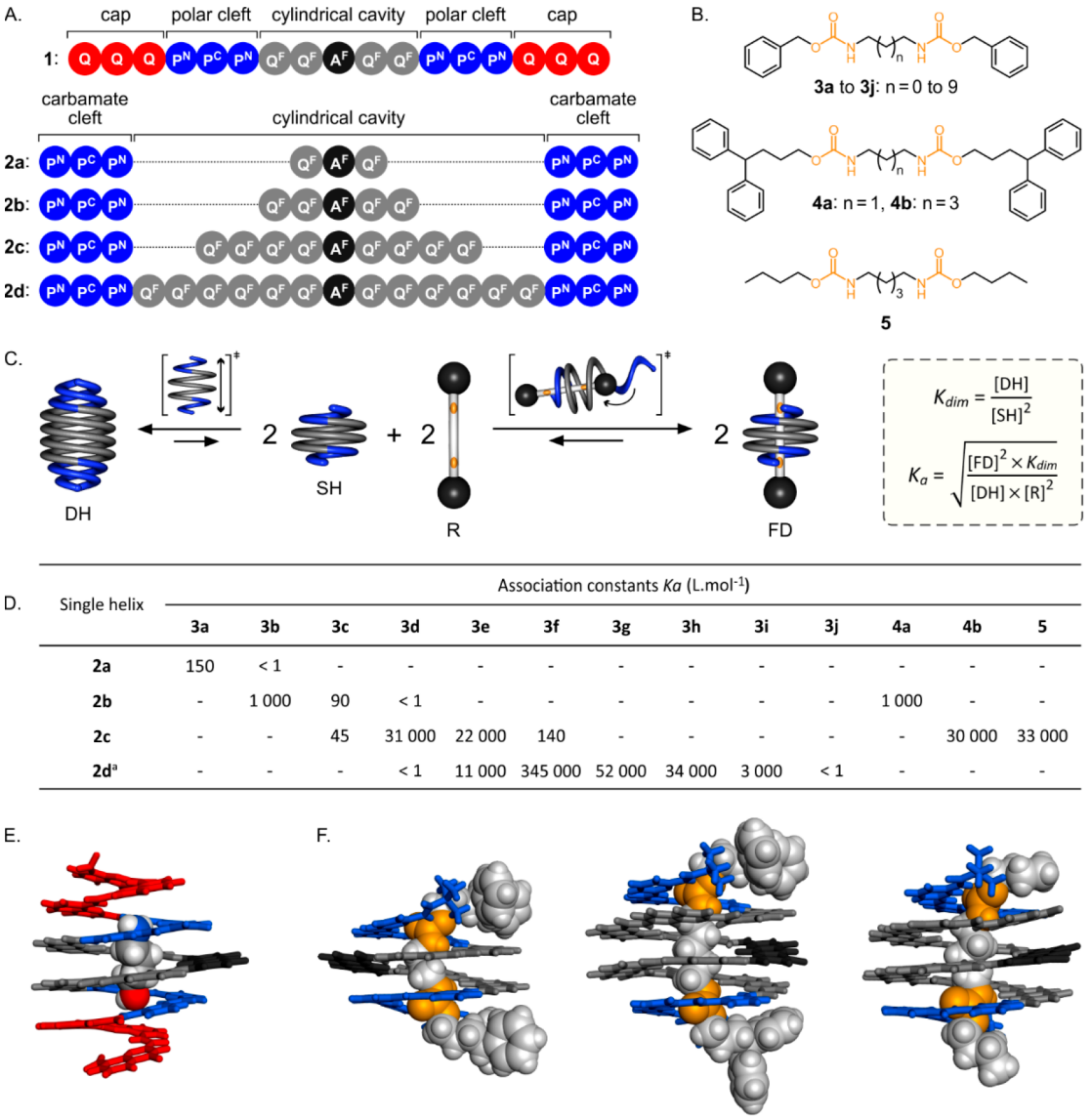

D.

Single helix	Association constants *Ka* (L.mol^{-1})												
	3a	**3b**	**3c**	**3d**	**3e**	**3f**	**3g**	**3h**	**3i**	**3j**	**4a**	**4b**	**5**
2a	150	< 1	-	-	-	-	-	-	-	-	-	-	-
2b	-	1 000	90	< 1	-	-	-	-	-	-	1 000	-	-
2c	-	-	45	31 000	22 000	140	-	-	-	-	-	30 000	33 000
2d[a]	-	-	-	< 1	11 000	345 000	52 000	34 000	3 000	< 1	-	-	-

Figure 3. (A) Sequences **1** and **2a**−**2d**. (B) Formulas of rod-like guests possessing two carbamate functional groups (orange) with bulky end groups (**3a**−**3j**, **4a**, **4b**) or without (**5**). (C) Equilibria between a dumbbell-shaped rod (R), a single (SH) or double (DH) helical foldamer, and a foldaxane (FD). (D) K_a values in $CDCl_3$ at 318 K of various foldaxanes and one pseudo-foldaxane, as determined by ^{1}H NMR spectroscopy. Crystal structures of complexes (E) **1**⊃4-amino-1-butanol and (F) **2b**⊃**4a**, **2c**⊃**4b**, and **2c**⊃**5**, from left to right. [a]For a homogeneous presentation, association constants (K_a) for **2d** have been recalculated at equilibrium using the equation proposed in panel C.

Double helix formation can thus be a practical impediment, but it can also be turned to an advantage. Just like double helical capsules have been produced,[52] we endeavored to design double helical foldaxanes. Sequences **8a**−**8c**, composed of a Q^F_n segment and a single $P^NP^CP^N$ segment were designed for this purpose (Figure 5A).[2,53,54] They assemble into double helical dimers in solution, which may be parallel or antiparallel. The latter configuration, in which one $P^NP^CP^N$ is found at each extremity of the duplex, was shown to produce double helical foldaxanes similar to the single helical foldaxanes presented above. The crystal structures of $(\mathbf{8a})_2$⊃**3b**, $(\mathbf{8a})_2$⊃**3d**, and $(\mathbf{8a})_2$⊃**3e** (Figure 5D) confirmed the stoichiometry, symmetry, and structure of these double-helical foldaxanes, in agreement with NMR data.[51] Again, a complex structural pathway must be invoked for the winding of a double helix around a dumbbell rod.

An interesting feature of these double helical foldaxanes is the lower dependence of their stability on the length of the rod than for single helical foldaxanes. The crystal structures of Figure 5D involve the same double helix, $(\mathbf{8a})_2$, and three different rods, and revealed that the two strands of the double helix may screw into one another to a variable extent to adjust their conformation to the guest. The structures of $(\mathbf{8c})_2$⊃**10a** and $(\mathbf{8c})_2$⊃**10b** (Figure 5F) also show an adjustment of the double helix to the length of the rod via screwing/unscrewing motions.[3] It follows that the transfer of a double helix from a guest to another guest of different length involves a screwing or unscrewing of the duplex (Figure 5C). This notion has relevance to controlled molecular motion because it combines a translation and a rotation, two motions that are generally dissociated in molecular systems.[55−58]

https://doi.org/10.1021/acs.accounts.2c00050
Acc. Chem. Res. 2022, 55, 1074−1085

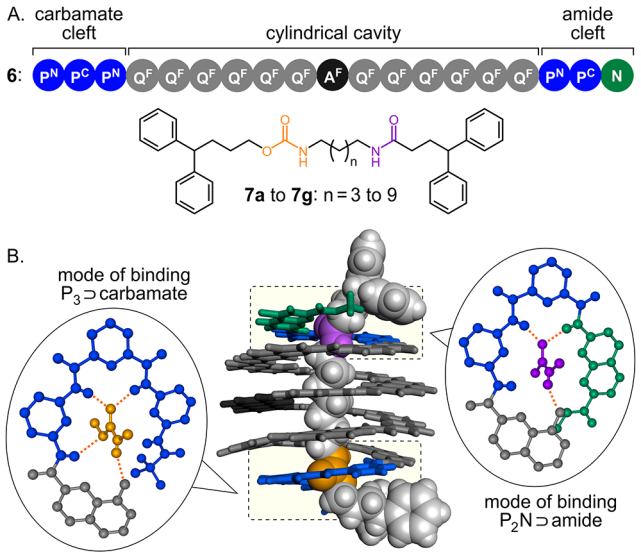

Figure 4. (A) Sequence of dissymmetrical helical foldamer **6** and formulas of dissymmetrical guests **7a**–**7g**. (B) Crystal structure of **6**⊃**7c** with magnification of the binding modes between either the $P^NP^CP^N$ cleft of the carbamate of the guest (left) or P^NP^CN of the amide (right).

4. SHUTTLING MOTIONS BASED ON FOLDAXANE ARCHITECTURES

The fact that helix winding around dumbbell rods to form foldaxanes takes place slowly, that is, on time scales ranging from minutes to days depending on their length, enabled their use in a manner similar to that of macrocycles in rotaxane-based molecular shuttles. Dumbbell-shaped rod **11a** was conceived for a proof-of-principle study (Figure 6A).[1] It contains two carbamate functions and one urea, that is, three hydrogen bond acceptors. Thus, **11a** possesses two binding stations but only one may be occupied at a given time. Solution and solid state data confirmed the exclusive formation of 1:1 single helical foldaxane **2c**⊃**11a**.[1] Using exchange NMR spectroscopy, it could be demonstrated that single helix **2c** transfers from one station to another and that this occurs at a rate (~3 min^{-1}) incompatible with the time necessary for unwinding (2 day^{-1}) and rewinding the helix.[1] Thus, actual sliding takes place without dissociation. Molecular dynamics simulations provided insights about energetic barriers and structural changes during the sliding process: on top of translation and rotations, the foldamer helix was also found to undergo a series of extensions and contractions.[59]

In the case of rod **11a**, the helix may move from one binding station to the other with equal probability. A step beyond consists in controlling this motion by triggering repulsive interactions for one station. We used dissymmetrical rod **11b** (Figure 6A), which possesses one carbamate/urea station with a heptyl segment (noted α) and another with a diethylamine

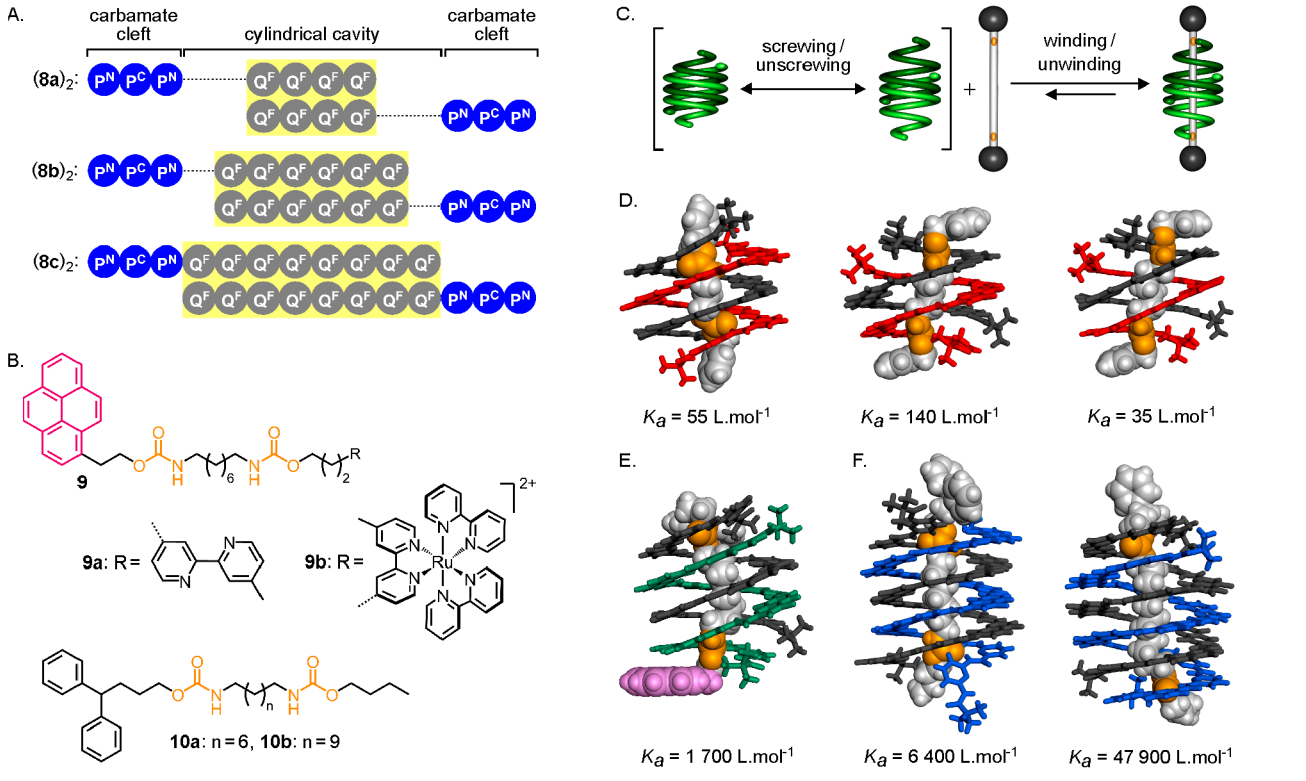

Figure 5. (A) Sequences of double-helical foldamers $(\mathbf{8a})_2$ to $(\mathbf{8c})_2$. (B) Formulas of dicarbamate guests. Guest **9b** is terminated by pyrene and $Ru(bpy)_3^{2+}$ chromophores (hexafluorophosphate counteranions are omitted for clarity). Guest **9a** is its precursor. Guests **10a** and **10b** possess only one bulky end group and thread themselves in double helix $(\mathbf{8c})_2$. (C) Formation of a [3]foldaxane from a double helix (green) wrapped around anchor points (orange) of a dumbbell-shaped rod. Crystal structures and association constants in $CDCl_3$ of foldaxanes (D) $(\mathbf{8a})_2$⊃**3b**, $(\mathbf{8a})_2$⊃**3d**, and $(\mathbf{8a})_2$⊃**3e** (left to right), (E) $(\mathbf{8b})_2$⊃**9a**, and (F) $(\mathbf{8c})_2$⊃**10a** and $(\mathbf{8c})_2$⊃**10b** (left to right). Doubles helices $(\mathbf{8a})_2$, $(\mathbf{8b})_2$, and $(\mathbf{8c})_2$ are shown in red/black, green/black, and blue/black, respectively.

https://doi.org/10.1021/acs.accounts.2c00050
Acc. Chem. Res. 2022, 55, 1074−1085

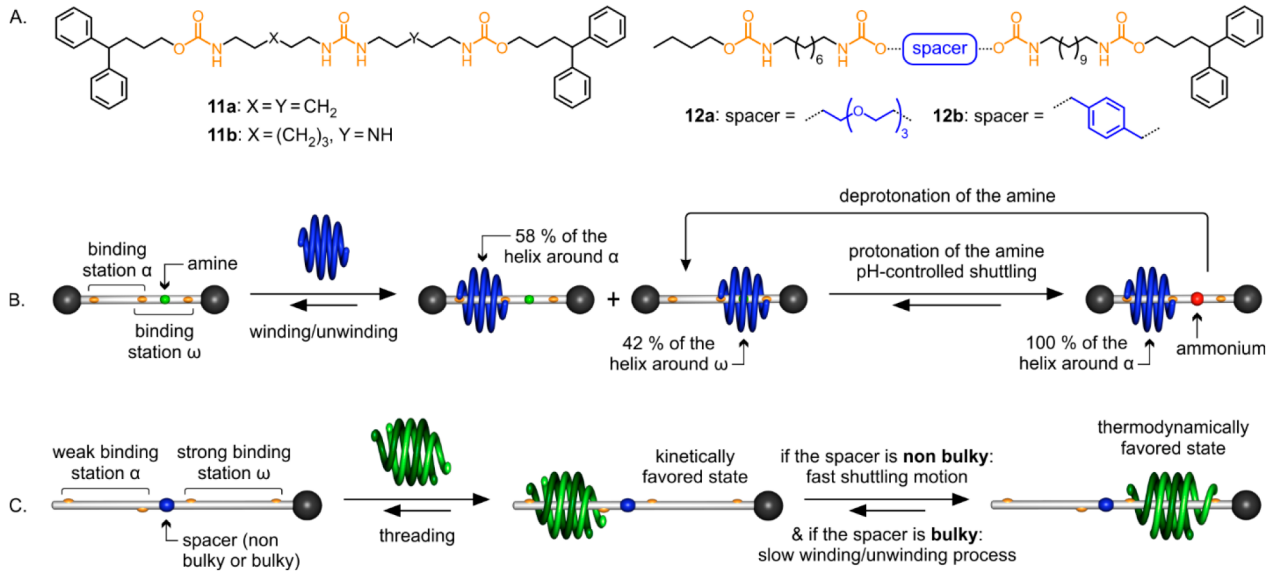

Figure 6. (A) Formulas of rods **11a**, **11b** and **12a**, **12b**. (B) Equilibria that govern the pH-controlled shuttling of single helix **2c** (blue) along rod **11b**. (C) Unidirectional fast shuttling (with a nonbulky spacer) or slow unwinding/rewinding (with a bulky spacer) of double helix $(\mathbf{8c})_2$ (green) from the α-station to the ω-station of rods such as **12a** (tetraethylene glycol spacer) or **12b** (*p*-xylyl spacer).

segment (noted ω). Single foldaxane **2c⊃11b** was produced, and its NMR spectrum showed two sets of signals with slightly different proportions (58:42) meaning that single helix **2c** spends a bit more time on one station than on the other. Upon titration of **2c⊃11b** with an acid to protonate the amine-containing station, one set of signals disappeared, and only one remained. This reflects the fact that helix **2c** is trapped around the α station and repelled from the ω station because the helix cavity does not accommodate the ammonium function (Figure 6B). Adding a base reverts the process, eventually producing a foldaxane-based pH-controlled molecular shuttle.

In a subsequent step, helix motions around rods were organized into kinetically controlled multistep pathways. We designed rod **12a** (Figure 6A) possessing successively an α-binding station known to have a weak affinity for double helix $(\mathbf{8c})_2$, a nonbulky spacer, an ω-binding station known to have a strong affinity for $(\mathbf{8c})_2$, and a bulky stopper.[3] Rod **12b** only differs from **12a** in that it has a bulky *p*-xylyl spacer. Upon addition of an excess of **12a** or **12b** to a solution of $(\mathbf{8c})_2$, NMR showed that a single new species was immediately and quantitatively formed that corresponds to the fast and quantitative threading of the double helix $(\mathbf{8c})_2$ around the α-station of the rod, leading to kinetic supramolecular products $(\mathbf{8c})_2$⊃**12a**-α and $(\mathbf{8c})_2$⊃**12b**-α, respectively (Figure 6C). Over time, the emergence of a second set of resonances was observed by NMR and attributed to the thermodynamic products $(\mathbf{8c})_2$⊃**12a**-ω and $(\mathbf{8c})_2$⊃**12b**-ω. Foldaxane $(\mathbf{8c})_2$⊃**12a**-ω was produced within ∼3 h, which indicates a shuttling motion. The tetraethylene glycol spacers do not hamper the passage of the helix. In contrast, $(\mathbf{8c})_2$⊃**12b**-ω took ∼15 days to form, indicating that the bulky spacer of **12b** imposes a dissociation of $(\mathbf{8c})_2$⊃**12b**-α and the rewinding of the helix around the ω-station (Figure 6C).[3] Similar pathways can also be implemented with control over the orientation of the rod and helix, using the building blocks shown in Figure 4.[43]

5. POLYFOLDAXANES AND HELIX HANDEDNESS CONTROL

The high stability of single and double helical foldaxanes and the match between helix and rod length invited the challenge of formation of polyfoldaxanes on rods that would possess multiple binding stations. Such assemblies might, for example, enable organization in space of various functional groups attached to each helical component. Double helix $(\mathbf{8b})_2$ binds to rod **13a**, which possesses a single dicarbamate binding station (Figure 7A, K_a = 1700 L·mol^{-1} in $CDCl_3$).[2] It also binds to longer dumbbell-shaped rods **13b** to **13d** (Figure 7A), possessing, respectively, two, three, and five binding stations identical to that of **13a**. This eventually produces polyfoldaxanes $(\mathbf{8b})_4$⊃**13b**, $(\mathbf{8b})_6$⊃**13c**, and $(\mathbf{8b})_{10}$⊃**13d** (Figure 7C), the latter having a length of 9.1 nm and a mass of 22 kDa.[2] Neither the host nor the guest possesses stereogenic centers. Thus, $(\mathbf{8b})_2$ exists as a racemate of right- (*P*) and left-handed (*M*) enantiomeric conformers. Upon assembly of multiple helices on a rod, diastereomeric complexes may result. For example, $(\mathbf{8b})_4$⊃**13b** may have *PP*, *MM*, or *PM* (*meso*) stereochemistry. However, ^{1}H NMR and crystallography demonstrate that the polyfoldaxanes are all homochiral. Only racemates of $(P\text{-}\mathbf{8b})_{2n}$⊃**13** and $(M\text{-}\mathbf{8b})_{2n}$⊃**13** are produced, indicating quantitative helix−helix handedness communication between the helices bound to the same rod. The different dicarbamate stations of **13b**−**13d** are separated by an ethylene glycol spacer, which plays an important role in polyfoldaxane design. Indeed, if the spacer between two binding stations is too short, steric hindrance between adjacent double helices may prevent all stations from being occupied. Conversely, if the spacer is too long, an absence of contacts between adjacent double helices would hamper helix−helix handedness communication.

In addition to relative helix−helix handedness control, absolute handedness control was achieved through the incorporation of a chiral group at both ends of a binding station. For example, rods **14a**-(*S*,*S*) and **14b**-(*S*,*S*) possess two (*S*) phenethyl groups (Figure 7A). Circular dichroism and ^{1}H

https://doi.org/10.1021/acs.accounts.2c00050
Acc. Chem. Res. 2022, 55, 1074−1085

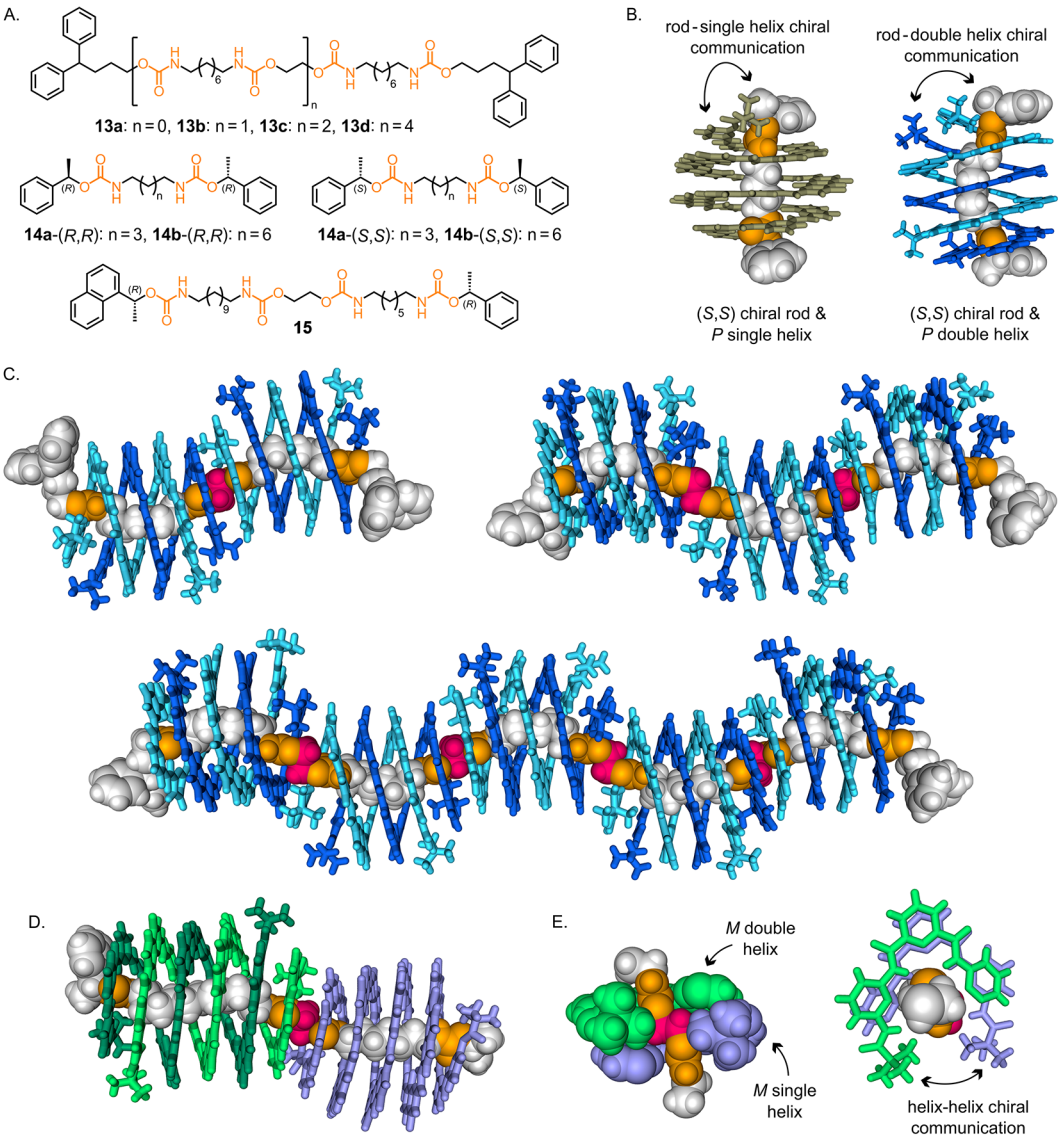

Figure 7. (A) Achiral rods **13a**−**13d** and chiral rods **14a**, **14b**, and **15**. (B) Crystal structures of *P*-**2c**⊃**14a**-(*S*,*S*) (left) and *P*-$(\mathbf{8b})_2$⊃**14b**-(*S*,*S*) (right) showing rod-to-helix chirality induction. (C) Crystal structures of polyfoldaxanes $(\mathbf{8b})_4$⊃**13b** (top, left), $(\mathbf{8b})_6$⊃**13c** (top, right) and energy-minimized molecular model, using MMFFs, of the [11]foldaxane $(\mathbf{8b})_{10}$⊃**13d** (bottom). (D) Crystal structure of the homochiral [4]foldaxane *M*-$(\mathbf{8c})_2$·*M*-**2d**⊃**15** with an enhanced view of the helix−helix interface (E). Helices **2c**, **2d**, $(\mathbf{8b})_2$, and $(\mathbf{8c})_2$ are colored in brown, purple, blue, and green, respectively. Carbamate groups and ethylene glycol spacers are represented in orange and pink, respectively.

NMR showed that the single helix **2c** binds to **14a**-(*S*,*S*) to give [2]foldaxane *P*-**2c**⊃**14a**-(*S*,*S*) with a de of 93%. Similarly, double helix $(\mathbf{8b})_2$ binds to **14b**-(*S*,*S*) to give [3]foldaxane *P*-$(\mathbf{8b})_2$⊃**14b**-(*S*,*S*) with a de of 56%. X-ray crystal structures allowed for the unambiguous assignment of the stereochemistry of these complexes (Figure 7B).

Geared toward template rods containing more information, compound **15** was made up successively of an (*R*)-naphthylethyl bulky group, a binding station known to bind $(\mathbf{8c})_2$, an ethylene glycol spacer, a binding station known to bind **2d**, and finally an (*R*)-chiral phenethyl bulky group (Figure 7A). Solution and solid state studies showed the formation of a homochiral [4]foldaxane, *M*-$(\mathbf{8c})_2$·*M*-**2d**⊃**15** (Figure 7D).[2] Additional rods made of multiple binding stations of variable lengths allowed for the faithful spatial arrangement of up to five single or double helices of three different kinds.[2] This type of assembly can be assimilated to a translation process where a sequence of alkyl carbamates is translated into a sequence of stacked aromatic helices. Translation of chemical information from one molecular type to another has reached exquisite levels in natural systems, for example, the translation of mRNA into proteins by the ribosome. In contrast, synthetic systems that achieve translation are few and far from being optimized.[60−62] The possibility to translate polycarbamates into aromatic oligoamides thus stands as an intriguing and original perspective.

6. EFFECT OF FOLDAXANE FORMATION ON ROD PROPERTIES

In all the systems presented above, foldaxane formation amounts to trapping an otherwise highly flexible guest containing an alkyl chain into the rigid cylindrical cavity of a multiturn aromatic helix. The extent of this rigidification, that is, how well does the helix keep the two ends of the guest away

https://doi.org/10.1021/acs.accounts.2c00050
Acc. Chem. Res. 2022, 55, 1074−1085

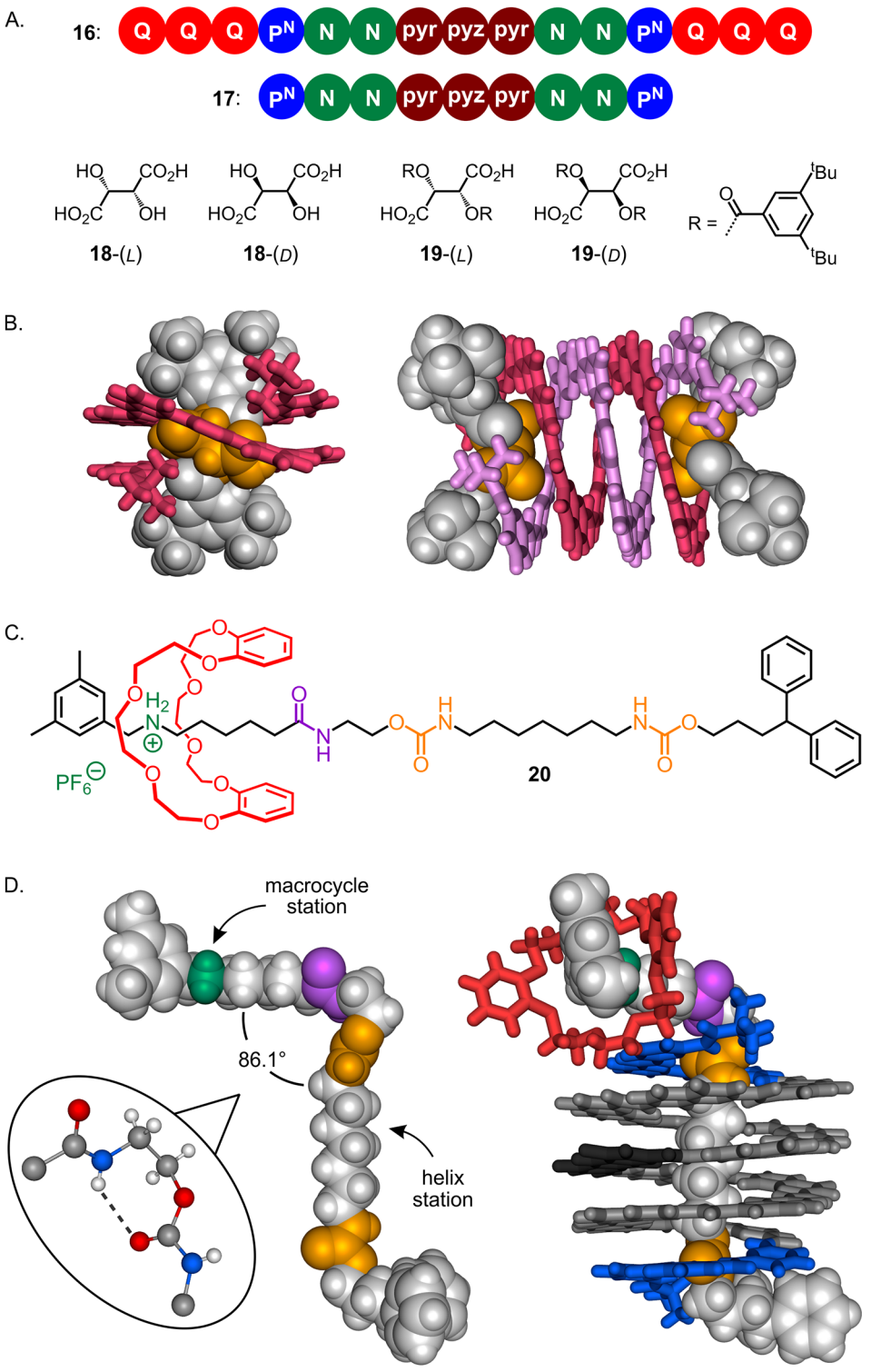

Figure 8. (A) Sequences of **16** and **17** and formulas of **18** and **19**. (B) Energy minimized molecular model, using MMFFs, of *M*-**17**⊃**19**-(L) (left) and crystal structure of $(P\text{-}\mathbf{17})_2\supset(\mathbf{19}\text{-}(\text{L}))_2$ (right). Tartaric acid moieties and bulky end groups are represented in orange and gray, respectively. (C) Formula of [2]rotaxane **20**. (D) Crystal structure of the foldarotaxane **2d**⊃**20** comprised of a DB24C8 macrocycle around an ammonium moiety and helix **2d** wrapped around a dicarbamate binding station; (left) enlarged view of the thread highlighting a kink due to a hydrogen bond between the amide (H-bond donor) and the central carbamate function (H-bond acceptor). The ammonium, amide, and carbamate functional groups are represented in green, dark purple, and orange, respectively. The macrocycle is shown in red, whereas the helix is color coded as in Figure 2.

from each other, was investigated using the distance dependence of reversible electronic energy transfer (REET).[52] To achieve this, a bulky $Ru(bpy)_3^{2+}$ (bpy = 2,2′-bipyridine) and a pyrene were installed at the ends of rod **9b** (Figure 5B) containing a binding station for $(\mathbf{8b})_2$. The emissive triplet metal to ligand charge transfer (^{3}MLCT) state of the

https://doi.org/10.1021/acs.accounts.2c00050
Acc. Chem. Res. 2022, 55, 1074−1085

$Ru(bpy)_3^{2+}$ chromophore is quasi-isoenergetic with the triplet state of the pyrene unit. This similarity allows the energy to shuttle back and forth between the two chromophores of the flexible thread all the more so that they can come in close proximity and a delayed luminescence was observed. After foldaxane formation, the chromophores are kept at a distance and effectively decoupled. Indeed, the structure of $(\mathbf{8b})_2\supset\mathbf{9a}$ shows an interchromophore distance ≥1.8 nm (Figure 5E). This translates into characteristic photophysical signatures.

Another intriguing interplay between helix and rod was discovered while extending foldaxane design to rods other than alkyl carbamate guests. Applying the same principles that led to the design of sequence **2** from the structure and molecular recognition properties of capsule **1** (Figure 3A), we endeavored to produce foldaxanes derived from the ability of capsule sequence **16** (Figure 8A) to bind to tartaric acid **18** with high affinity, selectivity, and diastereoselectivity ($K_a > 10^6$ $L{\cdot}mol^{-1}$ in $CDCl_3$/DMSO 99:1).[38] These molecular recognition properties stem from the larger cavity size of **16**, imparted by the long pyridine−pyridazine−pyridine central segment (Figure 2A) and from the presence of 7-amino-1,8-naphthyridine units, which hydrogen bond to the carboxylic acid guest. Thus, we synthesized sequence **17**, an analogue of **16** lacking terminal Q_3 caps while preserving molecular recognition features, and rod **19**, a dumbbell-shaped tartaric acid derivative.[63] Mixing **17** and **19** led to the rapid formation of the expected 1:1 foldaxane **17**⊃**19** (Figure 8B). There again, helix handedness was quantitatively biased by stereogenic centers of the guest. This complex was found to be long-lived, but it is in fact a kinetic supramolecular byproduct. Upon prolonged incubation, it slowly transformed into the 2:2 host−guest complex $(\mathbf{17})_2\supset(\mathbf{19})_2$ in which two guest molecules are bound at the extremities of a double helical $(\mathbf{17})_2$ (Figure 8B). We commented above that foldaxane formation most often outcompetes double helix formation (Figure 3C) because one duplex can produce two foldaxanes. This no longer holds true in the case of **17** and **19** because the rod-like guest also binds to the ends of the double helix through hydrogen-bonding (Figure 8B). Coincidentally, **19** also quantitatively biases the helicity of $(\mathbf{17})_2$ but with the opposite handedness to that it induces in **17**. Thus, mixing **17** and **19**-(L) leads first to the formation of *M*-**17**⊃**19**-(L) then to the formation of *P*-$(\mathbf{17})_2\supset(\mathbf{19}\text{-(L)})_2$.

Recent works exploited the fact that alkyl-carbamate rods that form foldaxanes may themselves be rotaxanes.[64] For instance, [2]rotaxane **20** (Figure 8C) possesses a dicarbamate binding station on which a helical foldamer may wind. It also contains an ammonium group as a binding site for a dibenzo-24-crown-8 (DB24C8) macrocycle. As evidenced by NMR, single helix **2d** wraps around the dicarbamate station of the rotaxane **20** to form **2d**⊃**20** (K_a = 207 000 $L{\cdot}mol^{-1}$ in $CDCl_3$), a new architecture, which was called a foldarotaxane. The crystal structure of **2d**⊃**20** confirms that each building block binds to its complementary interacting site (Figure 8D). Upon deprotonation of the ammonium, the macrocycle may occupy other locations of the rod. Helix **2d** still winds around the rod to form a foldarotaxane, but a significant decrease of affinity was observed (K_a = 9100 $L{\cdot}mol^{-1}$ in $CDCl_3$). The drop is even more pronounced upon subsequent *t*-butyl-carbamoylation of the amine (K_a = 3800 $L{\cdot}mol^{-1}$). Overall, the presence and the localization of the macrocycle modulates the association between the helix and the thread and, reciprocally, the foldamer can act as a supramolecular auxiliary to compartmentalize the macrocycle around a region of the molecular rod for which it may have a lesser affinity.

7. SUMMARY AND OUTLOOK

In summary, foldaxane development has made considerable progress owing to the use of designer aromatic oligoamide sequences. Structural parameters such as host−guest affinity and selectivity, host−guest relative orientation, and foldaxane single or double helicity, as well as relative and absolute handedness, can be controlled according to simple construction rules. Furthermore, the time scales of assembly and disassembly through different mechanisms and of various translation and screw-like molecular motions, can also be orchestrated by means of structural features. Foldaxanes thus extend earlier work on rotaxanes and pseudo-rotaxanes into new directions. Given the rich literature on molecular recognition within helical containers,[19−24] one may anticipate other foldaxanes than the alkyl-carbamate-guest/aromatic-oligoamide-host to emerge. In this respect, foldaxanes based on tartaric acid guests[61] or on helices not derived from aromatic amides[27−32] constitute early examples of a growing family. One may also conceive foldaxanes using other foldamer shapes than helices. For example, some aromatic bent sheets also possess a cavity.[65] The combination of rotaxanes and foldaxanes also has potential for development. An interesting prospect would be to use a foldamer helix as a controlled molecular auxiliary to confine another interlocked subunit (e.g., a macrocycle) along a molecular rod. Helix−rod host−guest complexes may also open new possibilities in the field of topologically complex molecules, e.g., knots. In a multiturn foldaxane, the helix and the rod are arranged with multiple crossing points. Upon appropriately covalently connecting the ends of the rod with the ends of the helix, a topologically nontrivial structure may result, as has been proposed for the synthesis of knots from double helices.[66,67] Progress along these lines is being made in our laboratories and will be reported in due course.

AUTHOR INFORMATION

Corresponding Authors

Ivan Huc − *Department Pharmazie, Ludwig-Maximilians-Universität, D-81377 München, Germany;* orcid.org/0000-0001-7036-9696; Email: ivan.huc@cup.lmu.de

Yann Ferrand − *CNRS, Bordeaux Institut National Polytechnique, CBMN (UMR 5248), Université de Bordeaux, Institut Européen de Chimie et Biologie, 33600 Pessac, France;* orcid.org/0000-0002-6552-6914; Email: yann.ferrand@u-bordeaux.fr

Authors

Victor Koehler − *CNRS, Bordeaux Institut National Polytechnique, CBMN (UMR 5248), Université de Bordeaux, Institut Européen de Chimie et Biologie, 33600 Pessac, France*

Arundhati Roy − *Department Pharmazie, Ludwig-Maximilians-Universität, D-81377 München, Germany*

Complete contact information is available at: https://pubs.acs.org/10.1021/acs.accounts.2c00050

https://doi.org/10.1021/acs.accounts.2c00050
Acc. Chem. Res. 2022, 55, 1074−1085

Author Contributions

[§]V. K. and A. R. contributed equally. The manuscript was written through contributions of all authors. All authors have given approval to the final version of the manuscript.

Funding

This work was supported by the Alexander von Humboldt foundation (postdoctoral fellowship to A.R.) and by the Agence Nationale de la Recherche (project ANR-17-CE07-0014-01).

Notes

The authors declare no competing financial interest.

Biographies

Victor Koehler received his M.Sc. degree in Molecular and Supramolecular Chemistry from the University of Strasbourg (France) in 2018. He then joined the Bio-Inspired Supramolecular Engineering laboratory at the Institute of Chemistry and Biology of Membranes and Nano-objects of the University of Bordeaux (France), headed by Dr. Yann Ferrand to carry out Ph.D. research. His work focuses on the design, synthesis, and characterization of a new class of self-assembled architectures called foldarotaxanes.

Arundhati Roy received her Ph.D. degree in Supramolecular Chemistry from IISER Pune (India) under the mentorship of Prof. Pinaki Talukdar in 2017. Following a 3-year postdoctoral experience with Prof. Huaqiang Zeng at A*STAR (Singapore), she moved to Ludwig-Maximilian-University, Munich, Germany, as an Alexander von Humboldt research fellow with Prof. Ivan Huc in 2020. Her current research interests focus on the development of aromatic foldamers for molecular recognition and transport.

Ivan Huc has been since 2017 a full Professor at the Ludwig-Maximilians-University (Munich, Germany). He obtained his doctorate from the University of Paris VI in 1994 for work performed jointly at Ecole Normale Supérieure (France) and MIT (USA). He subsequently worked as a postdoctoral researcher and then as CNRS researcher at the University of Strasbourg until 1998, when he was appointed group leader at the European Institute of Chemistry and Biology at the University of Bordeaux. His group focuses on the design, synthesis, and characterization of aromatic foldamers and their applications including pharmacological aspects.

Yann Ferrand is a CNRS research director and group leader at the Institute of Chemistry and Biology of Membranes and Nano-objects of the University of Bordeaux (France). He studied chemistry at the University of Rennes (France) where he received his Ph.D. degree in 2005. Then, he worked as a postdoctoral fellow in the School of Chemistry of the University of Bristol (United Kingdom) until 2007. His research focuses on the design and synthesis of synthetic macromolecules (e.g., foldamers) for the recognition of complex molecular targets and their use as sensors.

REFERENCES

(1) Gan, Q.; Ferrand, Y.; Bao, C.; Kauffmann, B.; Grélard, A.; Jiang, H.; Huc, I. Helix-Rod Host-Guest Complexes with Shuttling Rates Much Faster than Disassembly. *Science* **2011**, *331*, 1172−1175.

(2) Gan, Q.; Wang, X.; Kauffmann, B.; Rosu, F.; Ferrand, Y.; Huc, I. Translation of Rod-like Template Sequences into Homochiral Assemblies of Stacked Helical Oligomers. *Nat. Nanotechnol.* **2017**, *12*, 447−452.

(3) Wang, X.; Wicher, B.; Ferrand, Y.; Huc, I. Orchestrating Directional Molecular Motions: Kinetically Controlled Supramolecular Pathways of a Helical Host on Rodlike Guests. *J. Am. Chem. Soc.* **2017**, *139*, 9350−9358.

(4) Erbas-Cakmak, S.; Leigh, D. A.; McTernan, C. T.; Nussbaumer, A. L. Artificial Molecular Machines. *Chem. Rev.* **2015**, *115*, 10081−10206.

(5) Silvi, S.; Venturi, M.; Credi, A. Artificial Molecular Shuttles: From Concepts to Devices. *J. Mater. Chem.* **2009**, *19*, 2279−2294.

(6) Konstas, K.; Langford, S. J.; Latter, M. J. Advances Towards Synthetic Machines at the Molecular and Nanoscale Level. *Int. J. Mol. Sci.* **2010**, *11*, 2453−2472.

(7) Heard, A. W.; Goldup, S. M. Simplicity in the Design, Operation, and Applications of Mechanically Interlocked Molecular Machines. *ACS Cent. Sci.* **2020**, *6*, 117−128.

(8) Blight, B. A.; Van Noortwyk, K. A.; Wisner, J. A.; Jennings, M. C. [2]Pseudorotaxanes through Second-Sphere Coordination. *Angew. Chem., Int. Ed.* **2005**, *44*, 1499−1504.

(9) Loeb, S. J. Rotaxanes as Ligands: From Molecules to Materials. *Chem. Soc. Rev.* **2007**, *36*, 226−235.

(10) Xue, M.; Yang, Y.; Chi, X.; Yan, X.; Huang, F. Development of Pseudorotaxanes and Rotaxanes: From Synthesis to Stimuli-Responsive Motions to Applications. *Chem. Rev.* **2015**, *115*, 7398−7501.

(11) Bruns, C. J.; Stoddart, J. F. *The Nature of the Mechanical Bond: From Molecules to Machines*; Wiley, Hoboken, 2016.

(12) Ragazzon, G.; Baroncini, M.; Silvi, S.; Venturi, M.; Credi, A. Light-Powered Autonomous and Directional Molecular Motion of a Dissipative Self-Assembling System. *Nat. Nanotechnol.* **2015**, *10*, 70−75.

(13) Glink, P. T.; Oliva, A. I.; Stoddart, J. F.; White, A. J. P.; Williams, D. J. Template-Directed Synthesis of a [2]Rotaxane by the Clipping under Thermodynamic Control of a Crown Ether Like Macrocycle Around a Dialkylammonium Ion. *Angew. Chem., Int. Ed.* **2001**, *40*, 1870−1875.

(14) Chang, S.-Y.; Jang, H.-Y.; Jeong, K. S. Quantitative Comparison of Kinetic Stabilities of Metallomacrocycle-Based Rotaxanes. *Chem.—Eur. J.* **2003**, *9*, 1535−1541.

(15) Hunter, C. A.; Low, C. M.; Packer, M. J.; Spey, S. E.; Vinter, J. G.; Vysotsky, M. O.; Zonta, C. Noncovalent Assembly of [2]Rotaxane Architectures. *Angew. Chem., Int. Ed.* **2001**, *40*, 2678−2682.

(16) In earlier publications (e.g., ref 3), we referred to foldaxanes as a being sort of pseudo-rotaxane in the sense that they are rotaxane-like. However, the field generally restricts the term pseudo-rotaxane to the architectures shown in Figure 1B, comprised of a macrocycle and a rod without stoppers. We thus recommend the term rotaxane-like architectures to describe foldaxanes.

(17) Gellman, S. H. Foldamers: A Manifesto. *Acc. Chem. Res.* **1998**, *31*, 173−180.

(18) Rinaldi, S. The Diverse World of Foldamers: Endless Possibilities of Self-Assembly. *Molecules* **2020**, *25*, 3276.

(19) Goodman, C. M.; Choi, S.; Shandler, S.; DeGrado, W. F. Foldamers as Versatile Frameworks for the Design and Evolution of Function. *Nat. Chem. Biol.* **2007**, *3*, 252−262.

(20) Guichard, G.; Huc, I. Synthetic Foldamers. *Chem. Commun.* **2011**, *47*, 5933−5941.

(21) Ferrand, Y.; Huc, I. Designing Helical Molecular Capsules Based on Folded Aromatic Amide Oligomers. *Acc. Chem. Res.* **2018**, *51*, 970−977.

(22) Juwarker, H.; Suk, J.-M.; Jeong, K.-S. Foldamers with Helical Cavities for Binding Complementary Guests. *Chem. Soc. Rev.* **2009**, *38*, 3316−3325.

(23) Yamato, K.; Kline, M.; Gong, B. Cavity-containing, Backbone-Rigidified Foldamers and Macrocycles. *Chem. Commun.* **2012**, *48*, 12142−12158.

(24) Lautrette, G.; Wicher, B.; Kauffmann, B.; Ferrand, Y.; Huc, I. Iterative Evolution of an Abiotic Foldamer Sequence for the Recognition of Guest Molecules with Atomic Precision. *J. Am. Chem. Soc.* **2016**, *138*, 10314−10322.

(25) Horeau, M.; Lautrette, G.; Wicher, B.; Blot, V.; Lebreton, J.; Pipelier, M.; Dubreuil, D.; Ferrand, Y.; Huc, I. Metal-Coordination-Assisted Folding and Guest Binding in Helical Aromatic Oligoamide Molecular Capsules. *Angew. Chem., Int. Ed.* **2017**, *56*, 6823−6827.

https://doi.org/10.1021/acs.accounts.2c00050
Acc. Chem. Res. 2022, 55, 1074−1085

(26) Chang, K.-J.; Kang, B.-N.; Lee, M.-H.; Jeong, K.-S. Oligoindole-Based Foldamers with a Helical Conformation Induced by Chloride. *J. Am. Chem. Soc.* **2005**, *127*, 12214−12215.
(27) Hou, J. L.; Shao, X. B.; Chen, G. J.; Zhou, Y. X.; Jiang, X. K.; Li, Z. T. Hydrogen Bonded Oligohydrazide Foldamers and Their Recognition for Saccharides. *J. Am. Chem. Soc.* **2004**, *126*, 12386−12394.
(28) Ohishi, Y.; Abe, H.; Inouye, M. Native Mannose-Dominant Extraction by Pyridine-Phenol Alternating Oligomers Having an Extremely Efficient Repeating Motif of Hydrogen-Bonding Acceptors and Donors. *Chem.—Eur. J.* **2015**, *21*, 16504−16511.
(29) Meier, S.; Beeren, S. R. Simultaneous Determination of Binding Constants for Multiple Carbohydrate Hosts in Complex Mixtures. *J. Am. Chem. Soc.* **2014**, *136*, 11284−11287.
(30) Beeren, S. R.; Meier, S. Supramolecular Chemical Shift Reagents Inducing conformational Transitions: NMR Analysis of Carbohydrate Homooligomer Mixtures. *Chem. Commun.* **2015**, *51*, 3073−3076.
(31) Goto, K.; Moore, J. S. Sequence-Specific Binding of m-Phenylene Ethynylene Foldamers to a Piperazinium Dihydrochloride Salt. *Org. Lett.* **2005**, *7*, 1683−1686.
(32) Tanatani, A.; Hughes, T. S.; Moore, J. S. Foldamers as Dynamic Receptors: Probing the Mechanism of Molecular Association between Helical Oligomers and Rodlike Ligands. *Angew. Chem., Int. Ed.* **2002**, *41*, 325−328.
(33) Nishinaga, T.; Tanatani, A.; Oh, K.; Moore, J. S. The Size-Selective Synthesis of Folded Oligomers by Dynamic Templation. *J. Am. Chem. Soc.* **2002**, *124*, 5934−5935.
(34) Petitjean, A.; Cuccia, L. A.; Schmutz, M.; Lehn, J.-M. Naphthyridine-Based Helical Foldamers and Macrocycles: Synthesis, Cation Binding, and Supramolecular Assemblies. *J. Org. Chem.* **2008**, *73*, 2481−2495.
(35) Huc, I. Aromatic Oligoamide Foldamers. *Eur. J. Org. Chem.* **2004**, *2004*, 17−29.
(36) Zhang, D.-W.; Zhao, X.; Hou, J.-L.; Li, Z.-T. Aromatic Amide Foldamers: Structures, Properties, and Functions. *Chem. Rev.* **2012**, *112*, 5271−5316.
(37) Prabhakaran, P.; Priya, G.; Sanjayan, G. J. Foldamers: They're Not Just for Biomedical Applications Anymore. *Angew. Chem., Int. Ed.* **2012**, *51*, 4006−4008.
(38) Hua, Y.; Liu, Y.; Chen, C.-H.; Flood, A. H. Hydrophobic Collapse of Foldamer Capsules Drives Picomolar-Level Chloride Binding in Aqueous Acetonitrile Solutions. *J. Am. Chem. Soc.* **2013**, *135*, 14401−14412.
(39) Wang, W.; Zhang, C.; Qi, S.; Deng, X.; Yang, B.; Liu, J.; Dong, Z. A Switchable Helical Capsule for Encapsulation and Release of Potassium Ion. *J. Org. Chem.* **2018**, *83*, 1898−1902.
(40) Ferrand, Y.; Kendhale, A. M.; Kauffmann, B.; Grélard, A.; Marie, C.; Blot, V.; Pipelier, M.; Dubreuil, D.; Huc, I. Diastereoselective Encapsulation of Tartaric Acid by a Helical Aromatic Oligoamide. *J. Am. Chem. Soc.* **2010**, *132*, 7858−7859.
(41) Chandramouli, N.; Ferrand, Y.; Lautrette, G.; Kauffmann, B.; Mackereth, C. D.; Laguerre, M.; Dubreuil, D.; Huc, I. Iterative Design of a Helically Folded Aromatic Oligoamide Sequence for the Selective Encapsulation of Fructose. *Nat. Chem.* **2015**, *7*, 334−341.
(42) Mateus, P.; Chandramouli, N.; Mackereth, C. D.; Kauffmann, B.; Ferrand, Y.; Huc, I. Allosteric Recognition of Homomeric and Heteromeric Pairs of Monosaccharides by a Foldamer Capsule. *Angew. Chem., Int. Ed.* **2020**, *59*, 5797−5805.
(43) Bao, C.; Kauffmann, B.; Gan, Q.; Srinivas, K.; Jiang, H.; Huc, I. Converting Sequences of Aromatic Amino Acid Monomers into Functional Three-Dimensional Structures: Second-Generation Helical Capsules. *Angew. Chem., Int. Ed.* **2008**, *47*, 4153−4156.
(44) Qi, T.; Maurizot, V.; Noguchi, H.; Charoenraks, T.; Kauffmann, B.; Takafuji, M.; Ihara, H.; Huc, I. Solvent Dependence of Helix Stability in Aromatic Oligoamide Foldamers. *Chem. Commun.* **2012**, *48*, 6337−6339.
(45) Wang, X.; Gan, Q.; Wicher, B.; Ferrand, Y.; Huc, I. Directional Threading and Sliding of a Dissymmetrical Foldamer Helix on Dissymmetrical Axles. *Angew. Chem., Int. Ed.* **2019**, *58*, 4205−4209.
(46) Arduini, A.; Bussolati, R.; Credi, A.; Secchi, A.; Silvi, S.; Semeraro, M.; Venturi, M. Toward Directionally Controlled Molecular Motions and Kinetic Intra- and Intermolecular Self-Sorting: Threading Processes of Nonsymmetric Wheel and Axle Components. *J. Am. Chem. Soc.* **2013**, *135*, 9924−9930.
(47) Talotta, C.; Gaeta, C.; Qi, Z.; Schalley, C. A.; Neri, P. Pseudorotaxanes with Self-Sorted Sequence and Stereochemical Orientation. *Angew. Chem., Int. Ed.* **2013**, *52*, 7437−7441.
(48) Oshikiri, T.; Takashima, Y.; Yamaguchi, H.; Harada, A. Kinetic Control of Threading of Cyclodextrins onto Axle Molecules. *J. Am. Chem. Soc.* **2005**, *127*, 12186−12187.
(49) Nakamura, T.; Yamaguchi, G.; Nabeshima, T. Unidirectional Threading into a Bowl-Shaped Macrocyclic Trimer of Boron-Dipyrrin Complexes through Multipoint Recognition. *Angew. Chem., Int. Ed.* **2016**, *128*, 9758−9761.
(50) Berni, E.; Kauffmann, B.; Bao, C.; Lefeuvre, J.; Bassani, D. M.; Huc, I. Assessing the Mechanical Properties of a Molecular Spring. *Chem.—Eur. J.* **2007**, *13*, 8463−8469.
(51) Berni, E.; Garric, J.; Lamit, C.; Kauffmann, B.; Léger, J. M.; Huc, I. Interpenetrating Single Helical Capsules. *Chem. Commun.* **2008**, 1968−1970.
(52) Bao, C.; Gan, Q.; Kauffmann, B.; Jiang, H.; Huc, I. A Self-Assembled Foldamer Capsule: Combining Single and Double Helical Segments in One Aromatic Amide Sequence. *Chem.—Eur. J.* **2009**, *15*, 11530−11536.
(53) Ferrand, Y.; Gan, Q.; Kauffmann, B.; Jiang, H.; Huc, I. Template-Induced Screw Motions within an Aromatic Amide Foldamer Double Helix. *Angew. Chem., Int. Ed.* **2011**, *50*, 7572−7575.
(54) Denisov, S. A.; Gan, Q.; Wang, X.; Scarpantonio, L.; Ferrand, Y.; Kauffmann, B.; Jonusauskas, G.; Huc, I.; McClenaghan, N. D. Electronic Energy Transfer Modulation in a Dynamic Foldaxane: Proof-of-Principle of a Lifetime-Based Conformation Probe. *Angew. Chem., Int. Ed.* **2016**, *55*, 1328−1333.
(55) Muraoka, T.; Kinbara, K.; Aida, T. Mechanical Twisting of a Guest by a Photoresponsive Host. *Nature* **2006**, *440*, 512−515.
(56) Leigh, D. A.; Wong, J. K.; Dehez, F.; Zerbetto, F. Unidirectional Rotation in a Mechanically Interlocked Molecular Rotor. *Nature* **2003**, *424*, 174−179.
(57) Badjić, J. D.; Balzani, V.; Credi, A.; Silvi, S.; Stoddart, J. F. A Molecular Elevator. *Science* **2004**, *303*, 1845−1849.
(58) Jiménez, M. C.; Dietrich-Buchecker, C.; Sauvage, J. P. Towards Synthetic Molecular Muscles: Contraction and Stretching of a Linear Rotaxane Dimer. *Angew. Chem., Int. Ed.* **2000**, *39*, 3284−3287.
(59) Liu, P.; Hao, W.; Bian, X.; Mei, D. The Shuttling Mechanism of Foldaxanes: More than Just Translocation and Rotation. *Phys. Chem. Chem. Phys.* **2020**, *22*, 12967−12972.
(60) Lewandowski, B.; De Bo, G.; Ward, J. W.; Papmeyer, M.; Kuschel, S.; Aldegunde, M. J.; Gramlich, P. M. E.; Heckmann, D.; Goldup, S. M.; D'Souza, D. M.; Fernandes, A. E.; Leigh, D. A. Sequence-Specific Peptide Synthesis by an Artificial Small-Molecule Machine. *Science* **2013**, *339*, 189−193.
(61) He, Y.; Liu, D. R. Autonomous Multistep Organic Synthesis in a Single Isothermal Solution Mediated by a DNA Walker. *Nat. Nanotechnol.* **2010**, *5*, 778−782.
(62) McKee, M. L.; Milnes, P. J.; Bath, J.; Stulz, E.; Turberfield, A. J.; O'Reilly, R. K. Multistep DNA Templated Reactions for the Synthesis of Functional Sequence Controlled Oligomers. *Angew. Chem., Int. Ed.* **2010**, *49*, 7948−7951.
(63) Gan, Q.; Ferrand, Y.; Chandramouli, N.; Kauffmann, B.; Aube, C.; Dubreuil, D.; Huc, I. Identification of a Foldaxane Kinetic Byproduct during Guest-Induced Single to Double Helix Conversion. *J. Am. Chem. Soc.* **2012**, *134*, 15656−15659.
(64) Gauthier, M.; Koehler, V.; Clavel, C.; Kauffmann, B.; Huc, I.; Ferrand, Y.; Coutrot, F. Interplay between a Foldamer Helix and a Macrocycle in a Foldarotaxane Architecture. *Angew. Chem., Int. Ed.* **2021**, *60*, 8380−8384.

https://doi.org/10.1021/acs.accounts.2c00050
Acc. Chem. Res. 2022, 55, 1074−1085

(65) Atcher, J.; Mateus, P.; Kauffmann, B.; Rosu, F.; Maurizot, V.; Huc, I. Large Amplitude Conformational Changes in Self-Assembled Multi-Stranded Aromatic Sheets. *Angew. Chem., Int. Ed.* **2021**, *60*, 2574−2577.
(66) Dietrich-Buchecker, C. O.; Sauvage, J.-P. A Synthetic Molecular Trefoil Knot. *Angew. Chem., Int. Ed. Engl.* **1989**, *28*, 189−192.
(67) Ayme, J.-F.; Beves, J. E.; Campbell, C. J.; Leigh, D. A. Template Synthesis of Molecular Knots. *Chem. Soc. Rev.* **2013**, *42*, 1700−1712.

https://doi.org/10.1021/acs.accounts.2c00050
Acc. Chem. Res. 2022, 55, 1074−1085